








## Article

# A Comparative Overview of the Role of Human Ribonucleases in Nonsense-Mediated mRNA Decay

Paulo J. da Costa <sup>1,2,†</sup> , Juliane Menezes <sup>1,2,‡,§</sup> , Raquel Guedes <sup>1,2,||</sup> , Filipa P. Reis <sup>3</sup>, Alexandre Teixeira <sup>1,¶</sup>, Margarida Saramago <sup>3</sup> , Sandra C. Viegas <sup>3</sup> , Cecília M. Arraiano <sup>3,\*</sup>  and Luísa Romão <sup>1,2,\*</sup> 

- <sup>1</sup> Department of Human Genetics, National Institute of Health Dr. Ricardo Jorge, 1649-016 Lisbon, Portugal; pjgomes@unistra.fr (P.J.d.C.); julmenezes@ciencias.ulisboa.pt (J.M.); raqueldpguedes@gmail.com (R.G.); alexandre.teixeira.mgf@gmail.com (A.T.)
- <sup>2</sup> BioISI-Biosystems & Integrative Sciences Institute, Faculty of Sciences, University of Lisbon, 1749-016 Lisbon, Portugal
- <sup>3</sup> Instituto de Tecnologia Química e Biológica António Xavier, Universidade Nova de Lisboa, 2780-157 Oeiras, Portugal; anafilipareis@gmail.com (F.P.R.); margaridasaramago@itqb.unl.pt (M.S.); sviegas@itqb.unl.pt (S.C.V.)
- \* Correspondence: cecilia@itqb.unl.pt (C.M.A.); luisa.romao@insa.min-saude.pt (L.R.); Tel.: +351-214-469-547 (C.M.A.); +351-217-508-155 (L.R.)
- † Current address: Architecture et Réactivité de l'ARN, Institut de Biologie Moléculaire et Cellulaire, Université de Strasbourg, CNRS UPR9002, 2, Allée Konrad Roentgen, F-67084 Strasbourg, France.
- ‡ Current address: iNOVA4Health, Nova Medical School (NMS), Universidade Nova de Lisboa, 1150-190 Lisboa, Portugal.
- § Current address: cE3c—Centre for Ecology, Evolution and Environmental Changes & CHANGE—Global Change and Sustainability Institute, Departamento de Biologia Animal, Faculdade de Ciências, Universidade de Lisboa, 1749-016 Lisboa, Portugal.
- || Current address: iBET—Instituto de Biologia Experimental e Tecnológica, Av. República, Qta. do Marquês, 2780-157 Oeiras, Portugal.
- ¶ Current address: Unidade de Saúde Familiar-USF AlphaMouro—ULS-Amadora-Sintra, Av. Infante D. Henrique, 39–41, 1º Andar, 2635-367 Sintra, Portugal.



**Citation:** da Costa, P.J.; Menezes, J.; Guedes, R.; Reis, F.P.; Teixeira, A.; Saramago, M.; Viegas, S.C.; Arraiano, C.M.; Romão, L. A Comparative Overview of the Role of Human Ribonucleases in Nonsense-Mediated mRNA Decay. *Genes* **2024**, *15*, 1308. <https://doi.org/10.3390/genes15101308>

Academic Editors: Carlo Maria Di Liegro and Gabriella Schiera

Received: 29 August 2024  
Revised: 24 September 2024  
Accepted: 4 October 2024  
Published: 10 October 2024



**Copyright:** © 2024 by the authors. Licensee MDPI, Basel, Switzerland. This article is an open access article distributed under the terms and conditions of the Creative Commons Attribution (CC BY) license (<https://creativecommons.org/licenses/by/4.0/>).

**Abstract:** Eukaryotic cells possess surveillance mechanisms that detect and degrade defective transcripts. Aberrant transcripts include mRNAs with a premature termination codon (PTC), targeted by the nonsense-mediated decay (NMD) pathway, and mRNAs lacking a termination codon, targeted by the nonstop decay (NSD) pathway. The eukaryotic exosome, a ribonucleolytic complex, plays a crucial role in mRNA processing and turnover through its catalytic subunits PM/Sc1100 (Rrp6 in yeast), DIS3 (Rrp44 in yeast), and DIS3L1. Additionally, eukaryotic cells have other ribonucleases, such as SMG6 and XRN1, that participate in RNA surveillance. However, the specific pathways through which ribonucleases recognize and degrade mRNAs remain elusive. In this study, we characterized the involvement of human ribonucleases, both nuclear and cytoplasmic, in the mRNA surveillance mechanisms of NMD and NSD. We performed knockdowns of SMG6, PM/Sc1100, XRN1, DIS3, and DIS3L1, analyzing the resulting changes in mRNA levels of selected natural NMD targets by RT-qPCR. Additionally, we examined the levels of different human  $\beta$ -globin variants under the same conditions: wild-type, NMD-resistant, NMD-sensitive, and NSD-sensitive. Our results demonstrate that all the studied ribonucleases are involved in the decay of certain endogenous NMD targets. Furthermore, we observed that the ribonucleases SMG6 and DIS3 contribute to the degradation of all  $\beta$ -globin variants, with an exception for  $\beta$ NS in the former case. This is also the case for PM/Sc1100, which affects all  $\beta$ -globin variants except the NMD-sensitive variants. In contrast, DIS3L1 and XRN1 show specificity for  $\beta$ -globin WT and NMD-resistant variants. These findings suggest that eukaryotic ribonucleases are target-specific rather than pathway-specific. In addition, our data suggest that ribonucleases play broader roles in mRNA surveillance and degradation mechanisms beyond just NMD and NSD.

**Keywords:** mRNA surveillance; quality control; nonsense-mediated mRNA decay (NMD); nonstop decay (NSD); mRNA degradation; natural NMD targets

## 1. Introduction

The accumulation of nonfunctional RNAs is detrimental to the cell and has been linked to several human diseases [1,2]. Therefore, RNA quality control processes play a crucial role in recognizing and eliminating aberrant RNAs [3–7]. One such surveillance mechanism is nonstop mRNA decay (NSD). NSD detects mRNAs that lack a translation termination codon. In these mRNAs, the ribosome is able to read-through into the 3'-poly(A) tail, but in the poly(A) stretch, the ribosome slows down and stalls. The stalling of the ribosome leads to ribosome collisions, which are detected by the NSD machinery. Subsequent ribosome ubiquitination at the interface of two collided ribosomes is considered the signal for mRNA decay, which occurs through 3'-5' degradation by the exosome without prior deadenylation [4,8]. Conversely, transcripts with a premature translation termination codon (PTC) are detected and rapidly degraded by a different surveillance mechanism known as nonsense-mediated mRNA decay (NMD) [5,6]. By degrading mRNAs with nonsense codons, NMD prevents the synthesis of potentially deleterious C-terminally truncated proteins [5]. Interestingly, many physiological mRNAs, which possess features recognized by the NMD machinery, have also been identified as NMD substrates. This suggests an additional role for NMD as a posttranscriptional regulator of gene expression [9,10].

The degradation of NMD substrates involves both endonucleolytic and exonucleolytic activities [11]. Endonucleolytic degradation is catalyzed by SMG6, which cleaves the mRNA near the PTC. The resulting 5' and 3' RNA fragments are then quickly degraded by general cellular exonucleases [12,13]. In addition to the endonucleolytic route, mammalian cells possess alternative exonucleolytic decay pathways that involve deadenylation and decapping steps [5,11]. These pathways include SMG5-SMG7 or SMG5-PNRC2 proteins that further recruit the decapping complex (DCPC) and the deadenylation complex (CCR4-NOT) to remove the cap-binding complex and the poly(A) tail, allowing 5'-to-3' and 3'-to-5' RNA degradation by XRN1 and the RNA exosome, respectively [14–17]. Additionally, deadenylation-independent decapping and subsequent 5'-3' degradation also contribute to NMD [5,14–16].

The exosome is a multiprotein complex responsible for major 3'-5' RNA degradation in eukaryotes [18]. The eukaryotic core exosome is evolutionarily conserved and composed of 10 essential subunits found in both the nucleus and cytoplasm [19,20]. In yeast, only one of these subunits, DIS3, is responsible for the catalytic activity of the machinery [21,22]. As a member of the RNase II superfamily of exoribonucleases, DIS3 contains a conserved RNB domain responsible for the 3'-5' exoribonucleolytic activity of the exosome [23,24]. Additionally, DIS3 has endonucleolytic activity conferred by its PIN domain [25,26]. In humans, two homologues are part of the exosome: DIS3 and DIS3-like exoribonuclease 1 (DIS3L1) [27,28]. Both DIS3 and DIS3L1 are active 3'-5' exoribonucleases, but only DIS3 has endoribonuclease activity. Another difference between these two homologues is their subcellular localization. DIS3 primarily localizes in the nucleoplasm, with a small fraction in the cytoplasm, while DIS3L1 is exclusively localized in the cytoplasm [28].

DIS3L2, another member of the RNase II superfamily, is distinct from its counterparts. Unlike DIS3 and DIS3L1, DIS3L2 is not part of the exosome complex and is associated with an uridylation-dependent RNA degradation pathway [29–34]. Our lab has published a report on DIS3L2's role in the decay of natural NMD targets in a transcript-specific manner [35]. The involvement of DIS3L2 in NMD has also been reported by others [36].

Our understanding about the involvement of different human DIS3 exosome-associated homologues in RNA surveillance mechanisms remains limited. To investigate this, we evaluated the roles of DIS3 and DIS3L1, along with ribonucleases SMG6, PM/Sc1100, and XRN1, in the degradation of natural endogenous NMD targets. Our findings indicate that each of these ribonucleases contributes to the decay of at least one endogenous NMD target, highlighting their target-specific roles in NMD. Additionally, we explored their roles in the degradation of various human  $\beta$ -globin gene variants representing NSD and NMD-sensitive mRNAs. Our results show that the ribonucleases tested are not restricted

to a single mRNA decay pathway but also participate in the degradation of normal and/or NSD mRNAs, demonstrating a broader involvement in RNA turnover beyond NMD.

## 2. Materials and Methods

### 2.1. Plasmid Constructs

Each of the human  $\beta$ -globin gene variants  $\beta$ WT,  $\beta$ 15,  $\beta$ 26, and  $\beta$ 39 was obtained as previously described [37–39]. The NSD-sensitive variant  $\beta$ NS (nonstop) was obtained by site-directed mutagenesis at three sites: a TAA to AAA mutation at the natural stop codon and TAA to AAA and TGA to AGA mutations in the 3'UTR to eliminate any in-frame stop codons.

### 2.2. Cell Culture, Plasmid, and siRNA Transfections

HeLa cells were grown in Dulbecco's modified Eagle's medium (DMEM) supplemented with 10% fetal bovine serum and transiently transfected as previously described [35,40] using Lipofectamine 2000 reagent (Invitrogen, Carlsbad, CA, USA). All siRNA sequences are available in Supplementary Table S1. Twenty-four hours later, cells were harvested for RNA and protein expression analysis.

### 2.3. Isolation of Total RNA and Protein Lysates

Cells were lysed in NP40 buffer supplemented with Proteinase and RNase inhibitors to obtain protein extracts [35,40], and total RNA was extracted using the Nucleospin RNA extraction II Kit (Macherey-Nagel, Düren, Germany) following the manufacturer's indications.

### 2.4. Western Blot Analysis

Protein lysates were resolved on a 10% SDS-PAGE gel and transferred to polyvinylidene difluoride (PVDF) membranes (Bio-Rad, Hercules, CA, USA) following standard protocols. Membranes were probed with the following primary antibodies: mouse anti- $\alpha$ -tubulin (Sigma-Aldrich, Saint Louis, MO, USA; loading control) at 1:50,000 dilution, rabbit anti-XRN1 (Novus Biologicals, Centennial, CO, USA) at 1:500 dilution, rabbit anti-DIS3 (Sigma-Aldrich, Saint Louis, MO, USA) at 1:250 dilution, and rabbit anti-DIS3L1 (Sigma-Aldrich, Saint Louis, MO, USA) at 1:250 dilution. Subsequently, detection was carried out by incubating the membrane with the appropriate secondary antibodies: goat anti-rabbit horseradish peroxidase conjugate (Sigma-Aldrich, Saint Louis, MO, USA) diluted at 1:3000 and goat anti-mouse horseradish peroxidase conjugate (Bio-Rad) diluted at 1:4000 for  $\alpha$ -tubulin, followed by enhanced chemiluminescence.

### 2.5. Reverse Transcription, Semi-Quantitative PCR (sqPCR), and Real-Time PCR (RT-qPCR)

First-strand cDNA was synthesized from total RNA using reverse transcriptase (NZYtech) according to the manufacturer's instructions.

Semi-quantitative PCR for SMG6, PM/Scf100, and glyceraldehyde 3-phosphate dehydrogenase (GAPDH) cDNAs were performed under similar conditions: 3  $\mu$ L of the RT product was amplified in a 50  $\mu$ L reaction volume using 0.2 mM dNTPs, 15 pmol of each primer (Supplementary Table S2), 0.75 U of DreamTaq (Thermo Scientific, Waltham, MA, USA), and 1x PCR buffer (Thermo Scientific, MA, USA). The thermocycler conditions were 95 °C for 5 min, followed by 25–35 cycles of 94 °C for 30 s, 52–60 °C for 60 s, and 72 °C for 90 s, with a final extension of 72 °C for 5 min. Ten-microliter aliquots from each RT-PCR sample were analyzed by electrophoresis on 2% agarose gels.

RT-qPCR was performed with the ABI 7000 Sequence Detection System (Applied Biosystems, Foster City, CA, USA) using SYBR Green PCR Master Mix (Applied Biosystems), as previously described [35,40]. Ct values of the  $\beta$ -globin mRNA amplicons were compared to the respective  $\beta$ WT counterpart or to  $\beta$ WT at Luc siRNA conditions, as indicated in figures, and normalized with the reference amplicon Ct value. The forward and reverse primer sequences are available in Supplementary Table S2. Quantification was performed by the relative standard curve method and mRNA levels were determined by

RT-qPCR using primers specific for each natural NMD target and for GAPDH. All values are normalized to GAPDH mRNA levels [standard deviations are shown ( $n = 3$ , at least)].

## 2.6. Statistical Analysis

Statistical significance was assessed using one-way and two-way ANOVA, as appropriate. Significance levels were defined as follows: \*  $p < 0.05$ , \*\*  $p < 0.01$ , \*\*\*  $p < 0.001$ , and \*\*\*\*  $p < 0.0001$ . Results are presented as the mean  $\pm$  standard deviation from a minimum of three independent experiments.

## 3. Results

### 3.1. Human Ribonucleases Modulate the mRNA Levels of Different Natural NMD Targets

To study the impact of SMG6, PM/Scf100, DIS3, DIS3L1, or XRN1 on mRNA levels of natural NMD targets, we performed knockdowns (KDs) of each ribonuclease. As a positive control for NMD targeting, we knocked down UPF1, a key RNA helicase essential for initiation of the NMD pathway [41–48]. A siRNA targeting the luciferase mRNA sequence was used as a negative control (KD LUC). The KDs efficiency was monitored by sqPCR for SMG6 and PM/Scf100 and by Western blot analysis for UPF1, XRN1, DIS3, and DIS3L1 (Figure 1A). Subsequently, we assessed by RT-qPCR the effect of altering ribonuclease levels on the expression of selected natural NMD targets.

We selected 12 well-characterized natural NMD targets (*SMG5*, *SMG1*, *SLC7A11*, *GADD45A* and *B*, *GABARAPL1*, *ANTXR1*, *SLC1A3*, *PLXNA1*, *ATF3*, *ARFRP1*, and *BAG1*) and analyzed their mRNA levels in HeLa cells with and without depletion of ribonuclease genes (Figure 1). Fold-changes in mRNA levels are presented relative to control conditions (LUC siRNA-treated cells), which were arbitrarily set to 1.

Following the knockdown of the positive control gene UPF1, we observed a significant increase in mRNA levels for nearly all NMD targets studied, as expected, when compared to control conditions (Figure 1B).

Upon recognition by UPF1, NMD substrates can be degraded through various pathways. One known pathway involves the endonuclease SMG6, which, though primarily nuclear, also functions in the cytoplasm. SMG6 cleaves mRNA near the PTC, facilitating its degradation [12,13]. Depleting SMG6 resulted in substantial increases in the mRNA levels of nearly all analyzed natural NMD targets (Figure 1C). Specifically, *SMG5* and *SMG1* mRNA levels rose by approximately 2.0-fold and 1.7-fold, respectively. Both *SLC7A11* and *GADD45B* mRNA levels showed a 2.3-fold elevation, while *GADD45A* mRNA levels rose by 1.8-fold. *GABARAPL1* and *ANTXR1* mRNA levels elevated by 1.7-fold and 1.9-fold, respectively. Notably, *SLC1A3* mRNA increased substantially by 3.5-fold. *ARFRP1* accumulated by 1.9-fold and *BAG1* by 2.5-fold. This outcome was expected, as SMG6 is pivotal to the NMD process.

In the NMD pathway, after UPF1 initiates recognition and SMG6 induces endonucleolytic cleavage, the resulting mRNA fragments are targeted for subsequent exonucleolytic degradation from both the 5' and 3' ends. This degradation process involves recruiting decapping and 5'-to-3' exonuclease activities, as well as deadenylation and 3'-to-5' exonuclease activities.

The multiprotein complex exosome contains different catalytic subunits responsible for 3'-5' exonucleolytic RNA degradation, including PM/Scf100 (Rrp6 in yeast), DIS3 (Rrp44 in yeast), and DIS3L1. Silencing the nuclear RNase PM/Scf100 influenced the mRNA levels of four out of the twelve NMD targets analyzed (Figure 1D). The mRNA levels of *SMG5* and *GABARAPL1* were reduced by 0.7-fold. In contrast, *SLC7A11* and *SLC1A3* exhibited an increment of about 1.6-fold and 1.8-fold, respectively. These results suggest that while PM/Scf100 does not regulate the majority of the NMD transcripts tested, it may affect specific mRNAs.

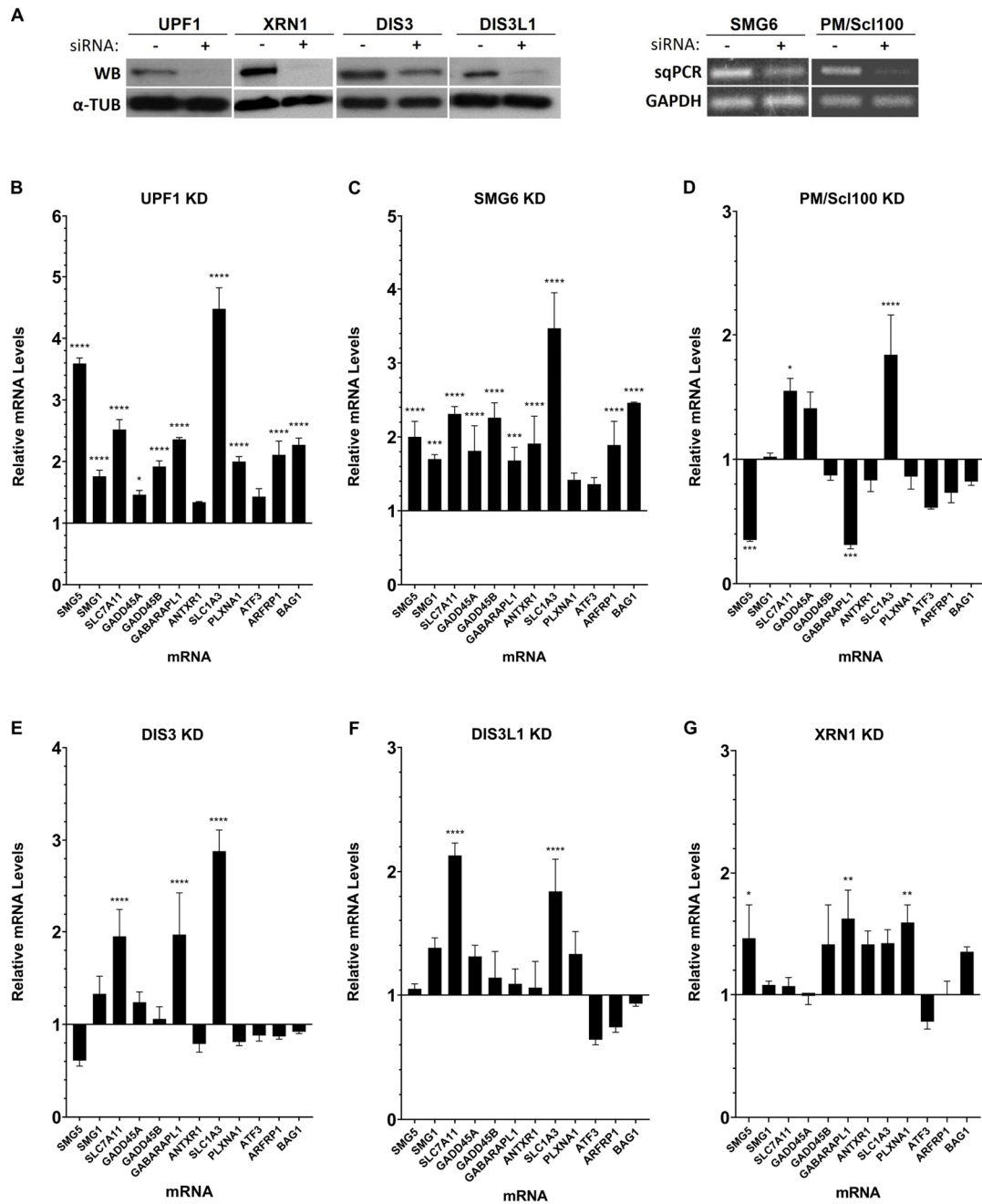


**Figure 1.** Human ribonucleases modulate the mRNA levels of different natural NMD targets. (A) Representative Western blot analysis of the UPF1, XRN1, DIS3, and DIS3L1 proteins and semi-quantitative PCR analysis of the *SMG6* and *PM/Scf100* mRNA levels extracted from HeLa cells with (+) or without (–) knockdown (KD), to monitor KD efficiency. (B–G) Real-time PCR (RT-qPCR) analysis of natural NMD targets in HeLa cells transiently transfected with Luciferase (LUC) siRNA (Control), UPF1, SMG6, PM/Scf100, DIS3, DIS3L1, or XRN1 siRNAs. The y-axis represents fold change, with a value of 1 indicating no change relative to the control. Values above 1 indicate upregulation, while values below 1 indicate downregulation. The control (Luciferase KD) was normalized to a baseline of 1, and all other conditions are shown relative to this baseline. Asterisks (\*) indicate statistical significance relative to the mRNA levels of the corresponding NMD target at control conditions: \*  $p < 0.05$ , \*\*  $p < 0.01$ , \*\*\*  $p < 0.001$ , and \*\*\*\*  $p < 0.0001$ .

Upon depletion of DIS3, another catalytic subunit of the exosome primarily localized in the nucleus, *SLC7A11* and *GABARAPL1* mRNA levels increased by 2.0-fold, and *SLCA3* mRNA levels rose by 2.9-fold compared to the control (Figure 1E).

Furthermore, the mRNA levels of *SLC7A11* and *SLC1A3* increased by 2.1-fold and 1.8-fold, respectively, when the cytoplasmic exoribonuclease DIS3L1, also a member of the exosome complex, was knocked down (Figure 1F).

Distinct from the exosome-mediated 3'-5' degradation, XRN1 is a key cytoplasmic enzyme involved in an alternative mRNA degradation pathway. As a 5'-3' exonuclease, XRN1 plays a crucial role in general mRNA turnover by processing mRNAs from the 5' end after decapping. Our study demonstrated that depletion of XRN1 led to the significant accumulation of *SMG5* mRNA by 1.5-fold and of both *GABARAP1* and *PLXNA1* mRNAs by 1.6-fold (Figure 1G).

In this section, we investigated the effects of depleting various human ribonucleases on the mRNA levels of known endogenous NMD targets to elucidate their roles in the NMD mechanism. Notably, none of the ribonucleases tested exhibited a general effect on the NMD targets. Instead, they appear to be involved in the degradation of specific NMD targets, revealing target specificity. Additionally, the 3'-5' exoribonucleases demonstrated redundancy over *SLC7A11* and *SLC1A13*, as both mRNAs can be degraded by all of them.

### 3.2. Roles of Human Ribonucleases in mRNA Surveillance Mechanisms: Use of Reporter Transcripts

To further elucidate the role of human ribonucleases in translation-dependent mRNA surveillance mechanisms such as NMD and NSD, we used the same genetic depletions as above: KD of *SMG6*, *PM/Scf100*, *DIS3*, *DIS3L1*, and *XRN1* (Figure 2). We transiently co-transfected HeLa cells depleted on each of these ribonucleases with constructs containing different human  $\beta$ -globin variants. These variants contain nonsense mutations in different codons of the  $\beta$ -globin gene that make the transcript  $\beta$ WT (wild type) become NMD-resistant ( $\beta$ 15), NMD-sensitive ( $\beta$ 26 and  $\beta$ 39), and NSD-sensitive ( $\beta$ NS) [37]. We assessed the changes in mRNA levels of all these different human  $\beta$ -globin variants by RT-qPCR.

We first analyzed the intrinsic effect in terms of mRNA accumulation levels of each of these variants under control conditions (LUC KD) (Appendix A). We observed a 1.3-fold increase in  $\beta$ 15 mRNA levels relative to  $\beta$ WT (arbitrarily set to 1), suggesting evasion of NMD. In contrast, the NMD-sensitive transcripts,  $\beta$ 26 and  $\beta$ 39, exhibited significant reductions to 0.6-fold of  $\beta$ WT levels, indicating that these transcripts are targeted for degradation by the NMD surveillance mechanism. The  $\beta$ NS mRNA levels decreased 0.3-fold. Throughout all experiments,  $\beta$ -globin mRNA levels in control conditions (LUC KD) consistently exhibited the same pattern, demonstrating the reproducibility of our system.

When we tested the KD of *SMG6* (Figure 2A) [12,13], we observed a significant increase in the mRNA levels of all  $\beta$ -globin variants, except  $\beta$ NS.

We also investigated the role of 3'-5' exonucleases, which generally act after endonucleolytic cleavage events. Specifically, we examined the nuclear exonuclease *PM/Scf100*, a component of the exosome complex, by measuring the mRNA levels of human  $\beta$ -globin variants following its depletion (Figure 2B). Our results indicate that *PM/Scf100* exhibits specificity for NMD-resistant and NSD-sensitive variants, with an increased mRNA fold-change variation for  $\beta$ WT (2.1-fold) and  $\beta$ 15 (3.3-fold), as well as  $\beta$ NS (0.7-fold) (Figure 2B). In contrast, the NMD-sensitive variants  $\beta$ 26 and  $\beta$ 39 were unaffected.

We conducted similar experiments to investigate the role of *DIS3*, a predominantly nuclear 3'-5' exonuclease, by measuring the mRNA levels of human  $\beta$ -globin variants following its KD (Figure 2C). Under these conditions, mRNAs of all  $\beta$ -globin variants, including  $\beta$ WT (20.7-fold),  $\beta$ 15 (22.1-fold),  $\beta$ 26 (4.2-fold),  $\beta$ 39 (4.8-fold), and  $\beta$ NS (3.4-fold), increased significantly compared to control conditions (Figure 2C). These results suggest that *DIS3* is not specific to any particular surveillance mechanism. However, its effect is notably more pronounced compared to other ribonucleases, leading to the largest increases in mRNA levels, particularly for the  $\beta$ WT and NMD-resistant variant ( $\beta$ 15).

Knockdown of the cytoplasmic 3'-5' exonuclease *DIS3L1* resulted in elevated mRNA levels of  $\beta$ -globin variants  $\beta$ WT (1.2-fold) and  $\beta$ 15 (2.1-fold) (Figure 2D). The levels of the NMD-sensitive variants  $\beta$ 26 and  $\beta$ 39 and of the NSD-sensitive variant,  $\beta$ NS, remained unchanged.

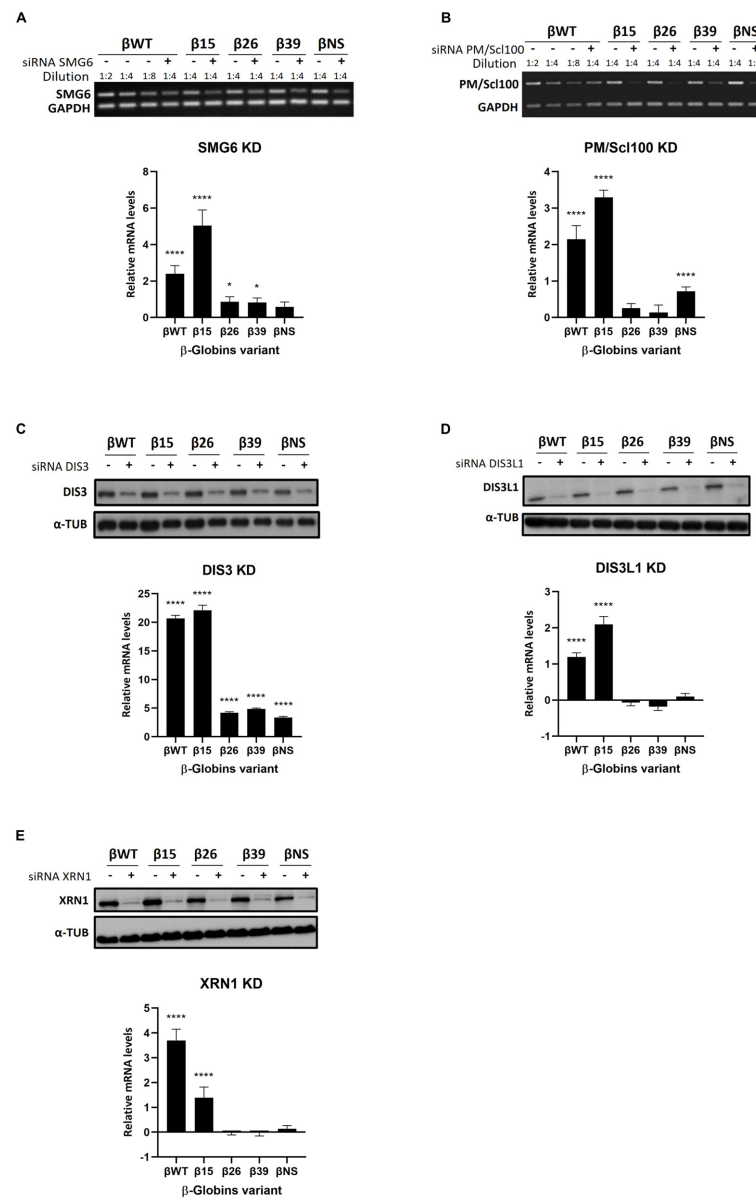


**Figure 2.** Human ribonucleases are involved in normal mRNA turnover as well as in the mRNA surveillance mechanisms of NMD and NSD. Representative semiquantitative PCR analysis of the *SMG6* (A) or *PM/Sc100* (B) mRNAs levels extracted from HeLa cells with (+) or without (–) knock-down (KD) and transiently transfected with plasmid-expressing wild type (βWT), NMD-resistant (β15), NMD-sensitive (β26 and β39), and NSD-sensitive (βNS) human β-globin mRNAs to monitor KD efficiency. (C–E) Representative Western blot analysis of protein extracted from HeLa cells with (+) or without (–) DIS3 and DIS3L1 KD and XRN1, respectively, and transiently co-transfected with plasmid-expressing βWT, β15, β26, β39, and βNS human β-globin mRNAs to monitor KD efficiency. (A–E) Real-time PCR (RT-qPCR) analysis of human β-globin mRNAs variants in HeLa cells transiently co-transfected with Luciferase (LUC) siRNA (Control), *SMG6*, *PM/Sc100*, *DIS3*, *DIS3L1*, or *XRN1* siRNAs. The *y*-axis represents the fold change in mRNA levels. Values above 0 indicate upregulation, while values below 0 indicate downregulation. To compare the impact of each ribonuclease knockdown (KD) relative to the control, the fold change observed under Luciferase KD was subtracted from the fold change observed under each ribonuclease KD. This adjustment highlights the additional effect of the ribonuclease KD on mRNA variations compared to the control condition. Asterisks (\*) indicate statistical significance relative to the mRNA levels of the corresponding NMD target under control conditions: \*  $p < 0.05$  and \*\*\*\*  $p < 0.0001$ .

A similar pattern was observed following the knockdown of the 5′-3′ cytoplasmic exoribonuclease XRN1 (Figure 2E). After XRN1 KD, mRNA levels of the  $\beta$ -globin variants  $\beta$ WT (3.7-fold) and  $\beta$ 15 (1.4-fold) increased significantly (Figure 2E). In contrast, XRN1 KD had minimal effects on the mRNA levels of the NMD-sensitive variants  $\beta$ 26 and  $\beta$ 39, as well as on the NSD-sensitive variant  $\beta$ NS, showing negligible differences from control levels (LUC KD). Our results suggest that both DIS3L1 and XRN1 exhibit some degree of specificity towards the  $\beta$ WT and the NMD-resistant variant  $\beta$ 15.

In summary, our study using  $\beta$ -globin variants, encompassing both NMD and NSD reporters, demonstrates that ribonucleases SMG6 and DIS3 play significant roles in the degradation of all  $\beta$ -globin variants, with an exception for  $\beta$ NS in the former case. PM/Scl100 specifically affects  $\beta$ -globin WT, as well as NMD-resistant and NSD-sensitive variants. Conversely, DIS3L1 and XRN1 show particular specificity for  $\beta$ -globin WT and NMD-resistant variants.

#### 4. Discussion

Eukaryotic cells have evolved various mRNA decay mechanisms to ensure proper mRNA processing and translatability. However, these mechanisms are more intricate than previously thought. Even within the well-studied mRNA quality control pathway of NMD, new details continue to emerge. The degradation of both normal and defective mRNAs is caused by ribonucleases, which are essential players in RNA decay processes. However, the specific roles and contributions of individual ribonucleases in these decay mechanisms remain unclear.

In this work, we investigated the roles of several human ribonucleases—SMG6, PM/Scl100, DIS3, DIS3L1, and XRN1—in the mRNA surveillance mechanisms of NMD and NSD. Building on our previous findings that depletion of DIS3L2 leads to significant accumulation of natural NMD targets [35,40], we aimed to further explore how these ribonucleases regulate the mRNA levels of 12 natural NMD targets: *SMG5*, *SMG1*, *SLC7A11*, *GADD45A*, *GADD45B*, *GABARAPL1*, *ANTXR1*, *SLC1A3*, *PLXNA1*, *ATF3*, *ARFRP1*, and *BAG1* [35,40,49] (data summarized in Table 1). Our study extended this investigation by also exploring their roles in aberrant mRNA turnover using a range of  $\beta$ -globin variants representing normal, NMD-sensitive, NMD-resistant, and NSD-sensitive mRNA forms (data summarized in Table 2). By comparing the effects of ribonuclease depletions on various targets, we aimed to uncover the mechanisms through which these proteins contribute to mRNA decay and surveillance processes.

**Table 1.** Summary of the observed effects on mRNA levels of endogenous NMD targets obtained under each ribonuclease knockdown.  $\uparrow$ —increase,  $\downarrow$ —decrease,  $\leftrightarrow$ —not affected.

Targets	Ribonucleases					
	SMG6 <sup>a</sup>	PM/Scl100 <sup>a</sup>	DIS3 <sup>a</sup>	DIS3L1 <sup>a</sup>	XRN1 <sup>a</sup>	DIS3L2 <sup>b</sup>
SMG5	$\uparrow$	$\downarrow$	$\leftrightarrow$	$\leftrightarrow$	$\uparrow$	$\leftrightarrow$
SMG1	$\uparrow$	$\leftrightarrow$	$\leftrightarrow$	$\leftrightarrow$	$\leftrightarrow$	$\uparrow$
SLC7A11	$\uparrow$	$\uparrow$	$\uparrow$	$\uparrow$	$\leftrightarrow$	$\uparrow$
GADD45A	$\uparrow$	$\leftrightarrow$	$\leftrightarrow$	$\leftrightarrow$	$\leftrightarrow$	$\uparrow$
GADD45B	$\uparrow$	$\leftrightarrow$	$\leftrightarrow$	$\leftrightarrow$	$\leftrightarrow$	$\uparrow$
GABARAPL1	$\uparrow$	$\downarrow$	$\uparrow$	$\leftrightarrow$	$\uparrow$	$\leftrightarrow$
ANTXR1	$\uparrow$	$\leftrightarrow$	$\leftrightarrow$	$\leftrightarrow$	$\leftrightarrow$	$\leftrightarrow$
SLC1A3	$\uparrow$	$\uparrow$	$\uparrow$	$\uparrow$	$\leftrightarrow$	$\uparrow$
PLXNA1	$\leftrightarrow$	$\leftrightarrow$	$\leftrightarrow$	$\leftrightarrow$	$\uparrow$	$\uparrow$
ATF3	$\leftrightarrow$	$\leftrightarrow$	$\leftrightarrow$	$\leftrightarrow$	$\leftrightarrow$	$\uparrow$
ARFRP1	$\uparrow$	$\leftrightarrow$	$\leftrightarrow$	$\leftrightarrow$	$\leftrightarrow$	$\leftrightarrow$
BAG1	$\uparrow$	$\leftrightarrow$	$\leftrightarrow$	$\leftrightarrow$	$\leftrightarrow$	$\leftrightarrow$

<sup>a</sup> this work; <sup>b</sup> [35].

**Table 2.** Summary of the observed effects on mRNA levels of the human  $\beta$ -globin variants obtained under each ribonuclease knockdown. ( $\beta$ WT) wild type, ( $\beta$ 15) NMD-resistant, ( $\beta$ 26 and  $\beta$ 39) NMD-sensitive, and ( $\beta$ NS) NSD-sensitive.  $\uparrow$ —increase,  $\leftrightarrow$ —not affected.

Targets	SMG6	PM/Scl100	DIS3	DIS3L1	XRN1
$\beta$ WT	$\uparrow$	$\uparrow$	$\uparrow$	$\uparrow$	$\uparrow$
$\beta$ 15	$\uparrow$	$\uparrow$	$\uparrow$	$\uparrow$	$\uparrow$
$\beta$ 26	$\uparrow$	$\leftrightarrow$	$\uparrow$	$\leftrightarrow$	$\leftrightarrow$
$\beta$ 39	$\uparrow$	$\leftrightarrow$	$\uparrow$	$\leftrightarrow$	$\leftrightarrow$
$\beta$ NS	$\leftrightarrow$	$\uparrow$	$\uparrow$	$\leftrightarrow$	$\leftrightarrow$

All the genes tested in this work play pivotal roles in various cellular processes. SMG5 and SMG1 are core components of the NMD machinery, SMG5 being involved in the degradation of NMD targets and SMG1 acting as a kinase that phosphorylates UPF1, initiating the NMD process [50,51]. SLC7A11 and SLC1A3 are involved in amino acid transport and neurotransmitter cycling, respectively, and their expression is tightly regulated to maintain cellular homeostasis [52,53]. GADD45A and GADD45B are stress response genes that mediate DNA repair and cell cycle control, crucial for preventing genomic instability [54]. GABARAPL1 is implicated in autophagy [55], while ANTXR1 plays a role in cell adhesion and immune response [56]. PLXNA1 guides axon growth and cell migration, and ATF3 is a transcription factor involved in stress response [57]. ARFRP1 regulates intracellular trafficking [58], and BAG1 is a co-chaperone that influences cell survival and apoptosis [59]. NMD ensures the fidelity of gene expression in these natural mRNAs, since they have features that can induce premature translation termination. This degradation process controls protein levels according to cellular needs, preventing the production of abnormal amounts of protein that could disrupt cellular function and contribute to disease.

In general, surveillance mechanisms exist both in the nucleus and the cytoplasm to detect errors at all stages of mRNA production and maturation. In this study, we tested the involvement of the nuclear ribonucleases PM/Scl100 and DIS3, as well as the cytoplasmic ribonucleases DIS3L1 and XRN1, in these mechanisms. Additionally, we investigated SMG6, which functions in both the nucleus and cytoplasm.

The SMG6 has long been recognized as a crucial endoribonuclease in the NMD surveillance mechanism, often referred to as the “long sought NMD endonuclease” [12], a concept consistently supported by numerous studies [60–63]. SMG6 functions by cleaving mRNAs near PTCs, initiating the degradation process essential for NMD [61]. Our data show that SMG6 knockdown leads to increased mRNA levels for almost all the studied NMD targets (10 out of 12) (Figure 1; Table 1). These results not only reaffirm the well-documented function of SMG6 in the NMD pathway but also validate our experimental system. SMG6 KD also causes elevated mRNA levels for two of the  $\beta$ -globin variants, WT and NMD-resistant form  $\beta$ 15 (Figure 2 and Table 2). This aligns with previous evidence showing that SMG6 is involved in the decay of mRNAs, even if they do not display NMD-inducing features [64,65]. Accordingly, Metzger and colleagues (2013) demonstrated that SMG6 knockdown increases the mRNA levels of PTC-free reporter gene variants [64]. Additionally, Nicholson et al. (2014) found that tethering SMG6 to an mRNA lacking NMD features significantly reduces its mRNA levels [65].

In the nucleus, defective mRNAs arising from errors in transcription or maturation are targeted for degradation. Both 3' to 5' and 5' to 3' pathways contribute to nuclear mRNA turnover. The exosome complex, a critical player in this process, relies on ribonucleases DIS3 and PM/Scl100 for its 3'-5' RNA degradation activity. During mRNA maturation in the nucleus, which includes splicing and the addition of a poly(A) tail, the exosome degrades improperly processed mRNAs, such as those that are un-spliced or have defective polyadenylation [6,7].

DIS3 is predominantly a nuclear ribonuclease (with some presence in the cytoplasm) and functions as both a 3'-5' exoribonuclease and endoribonuclease within the nuclear

exosome. Initially discovered in yeast for its role in ribosomal RNA (rRNA) processing [19], DIS3 and the exosome were later found to be involved in mRNA quality control mechanisms such as NMD and general mRNA turnover in yeast cells. However, its activity was reported to not be required for the degradation of NSD mRNAs [6,7,12,66–69]. It remains to be elucidated whether the DIS3 exosome component has a direct role in the degradation of mRNAs in mammalian cells, specifically those targeted by surveillance pathways. To address this, we investigated DIS3-depleted cells and found that only three of the measured mRNAs—*SLC7A11*, *GABARAPL1*, and *SLC1A3*—accumulated (Figure 1; Table 1). This suggests that most of the NMD targets tested do not require DIS3 for their degradation. Additionally, DIS3 knockdown substantially increased the mRNA levels of all  $\beta$ -globin variants, with a more pronounced effect on the WT and NMD-resistant  $\beta$ -globin variants (Figure 2; Table 2). The observation that the NMD- and NSD-sensitive variants are less affected aligns with the fact that both NMD and NSD are generally considered cytoplasmic processes, whereas DIS3 is predominantly localized in the nucleus. However, the depletion of DIS3 resulted in significantly higher expression levels of all  $\beta$ -globin variant mRNAs compared to the other ribonuclease knockdowns. In the nucleus, DIS3 is known to maintain RNA polymerase II transcriptome homeostasis and control widespread transcription initiation and premature termination [70]. Therefore, we attribute the observed effect to DIS3's association with RNA polymerase II and its role in ensuring the rapid degradation of unwanted RNAs. This accumulation likely results from the buildup of these species, which can exceed the levels of mature mRNAs, thereby contributing to the observed mRNA increase [71,72]. Overall, our study indicates that while DIS3 does not play a major role in NMD, it is directly involved in the decay of certain specific NMD targets. Moreover, this ribonuclease appears to maintain normal levels of the  $\beta$ -globin mRNA reporters: WT and NMD-resistant.

PM/Scl100, also known as EXOSC10, is a nuclear ribonuclease with 3'-5' exoribonucleolytic activity involved in the degradation of various RNA species, including normal and PTC-containing mRNAs, as well as structured RNAs such as rRNAs, small nuclear RNAs (snRNAs), and small nucleolar RNAs (snoRNAs) [14,73–75]. Our data indicate that PM/Scl100 has a limited impact on most natural NMD target mRNAs (Figure 1; Table 1). Exceptions include the increased mRNA levels of *SLC7A11* and *SLC1A3*, which may result from the inhibition of nuclear degradation of their corresponding pre-mRNAs, leading to transcript accumulation. Conversely, a reduction in mRNA levels was observed for certain NMD targets, with a more pronounced effect on *SMG5* and *GABARAPL1* mRNAs. This reduction likely reflects an indirect effect, as PM/Scl100 may influence other regulatory factors involved in controlling these mRNAs. Additionally, PM/Scl100 affects the mRNA levels of the  $\beta$ WT, the NMD-resistant  $\beta$ 15 variant, and the NSD-sensitive  $\beta$ NS, while NMD-sensitive variants ( $\beta$ 26 and  $\beta$ 39) remain unaffected (Figure 2; Table 2). To our knowledge, this study provides the first evidence linking PM/Scl100 to the degradation of NSD targets. In yeast, the PM/Scl100 homolog Rrp6 acts as a channel gate, enhancing Dis3's catalytic activity within the exosome's central channel and stimulating both exo- and endoribonuclease activities of Dis3 [76–78]. Our findings suggest that the effects observed in WT  $\beta$ -globin and NMD-resistant variants are likely due to the combined inhibition of PM/Scl100 and the resultant decrease in DIS3 catalytic activity. However, this does not fully explain why NMD-sensitive mRNAs ( $\beta$ 26 and  $\beta$ 39) remain unaffected (Figure 2C). One possible explanation is that, despite reduced nuclear degradation of these NMD-sensitive variants due to PM/Scl100 silencing and diminished DIS3 activity, cytoplasmic surveillance mechanisms might compensate for the increased levels of these mRNAs that have been exported to the cytoplasm.

XRN1 is a major cytoplasmic 5'-3' exoribonuclease responsible for degrading mRNAs following the removal of their 5' cap, a process known as decapping, which makes the RNA susceptible to degradation. This ribonuclease is well-documented for its involvement in bulk mRNA degradation [79,80], as well as in the decay of intermediates in NSD and NMD [79,81,82]. Our study further reveals that XRN1 depletion affects the mRNA levels

of 3 out of 12 tested natural NMD targets (*SMG5*, *GABARAPL1*, and *PLXNA1*) (Figure 1; Table 1). This finding confirms that XRN1 is involved in NMD target degradation. However, it does not appear to be essential for the decay of all NMD targets. The variability observed among different NMD targets could be attributed to specific features that either inhibit decapping or interfere with XRN1-mediated degradation, like what has been observed with some viral RNAs [83,84]. Additionally, XRN1 targets both  $\beta$ WT and NMD-resistant  $\beta$ -globin variants but does not significantly affect the NMD- and NSD-sensitive variants.

Unlike XRN1's 5'-3' degradation pathway, the exosome complex utilizes the alternative 3'-5' degradation pathway for RNA decay, with different exosome-associated ribonucleases operating depending on the cellular location of the complex [40]. DIS3L1 is a cytoplasmic exosome component with 3'-5' exoribonucleolytic activity. This ribonuclease has been primarily studied in yeast, with limited research in mammalian cells revealing its involvement in rRNA degradation and the accumulation of polyadenylated rRNA intermediates upon its depletion [27,28]. Our study advances current understanding by demonstrating that DIS3L1 plays a role in the decay of mRNAs encoding natural NMD targets, such as *SLC7A11* and *SLC1A3* (Figure 1; Table 1). We also observed that depleting DIS3L1 leads to increased mRNA levels for the WT  $\beta$ -globin and NMD-resistant ( $\beta$ 15) variants (Figure 2; Table 2). Therefore, our findings reveal that DIS3L1 exhibits target specificity within the NMD pathway, affecting certain targets but not others. Also, this research is the first to provide evidence of DIS3L1's involvement in specific RNA decay processes.

DIS3L2, unlike its DIS3 family counterparts (DIS3 and DIS3L1), is not part of the exosome and is involved in cytoplasmic RNA degradation pathways, particularly those involving uridylation-dependent RNA decay mechanisms. This process relies on the addition of untemplated uridine residues to mRNAs and other RNA classes by terminal uridylyl transferases (TUTases). Our previous research has shown that nearly half of the natural NMD targets tested in this study are substrates of DIS3L2 in human cells (Table 1) [35]. These targets include *SMG1*, *SLC7A11*, *GADD45A*, *GADD45B*, *SLC1A3*, *PLXNA1*, and *ATF3*. Consequently, among all the ribonucleases discussed in this work, DIS3L2 appears to have the most significant impact on NMD transcripts.

Overall, we found that human ribonucleases, whether localized in the nucleus and/or cytoplasm, exhibit selectivity for specific natural NMD targets. This selectivity appears to be influenced by the unique characteristics of each transcript, such as its sequence and length, G, C, A, and U relative content, secondary structure, etc. Despite target specificity, our findings also indicate the existence of functional redundancy among these ribonucleases. For instance, we observed that mRNA levels of *SLC7A11* and *SLC1A3* accumulate following the knockdown of the 3'-5' exonucleases PM/Sc100, DIS3, DIS3L1, and DIS3L2. This functional redundancy might be due to a common feature observed in the different target transcripts. In contrast, these mRNAs are not affected by the 5'-3' exonuclease XRN1. Additionally, we found that these ribonucleases are involved in the decay of normal mRNAs and, beyond NMD, participate in other surveillance pathways such as NSD. Together, our results show that ribonucleases act specifically on certain mRNA targets, but multiple ribonucleases function redundantly. The interplay between specificity and redundancy may be explained by the presence of single or multiple and exclusive or shared transcript features, respectively. As an example, the 3'-end uridylation of specific RNAs makes them Dis3L2 targets [29–34]. Nevertheless, a more detailed mechanistic understanding of this interplay is of great interest for investigation in the future.

## 5. Conclusions

Transcriptome-wide analyses have revealed that NMD modulates ~10% of human cell mRNAs [9]. Understanding how ribonucleases regulate subsets of NMD targets could reveal new therapeutic approaches for diseases such as cancer, where NMD pathway dysregulation plays a significant role. The understanding of their involvement in NSD is also important, since it also plays a role in the etiology of some genetic disorders [85,86].

Our findings provide a comprehensive overview of how different human ribonucleases influence the stability of transcripts targeted by the surveillance mechanisms of NMD and NSD. In these pathways, they reveal some redundancy between them and act in a target-specific manner. We show that ribonucleases are not confined to specific surveillance pathways but play broader roles in mRNA surveillance and turnover.

**Supplementary Materials:** The following supporting information can be downloaded at <https://www.mdpi.com/article/10.3390/genes15101308/s1>. Table S1: siRNAs used in this work; Table S2: Oligonucleotides used in this work.

**Author Contributions:** P.J.d.C. and J.M. performed the experiments, analyzed the results, and wrote the draft of the manuscript. R.G. performed the experiments for SMG6 and PM/Scf100. F.P.R. performed preliminary experiments. M.S. and S.C.V. analyzed the data and prepared the final version of the manuscript. A.T., C.M.A. and L.R. designed the project, evaluated the experimental results, and revised the manuscript. All authors have read and agreed to the published version of the manuscript.

**Funding:** This work was partially supported by Instituto Nacional de Saúde Doutor Ricardo Jorge and Fundação para a Ciência e a Tecnologia (FCT), Portugal [UIDB/04046/2020 (DOI: 10.54499/UIDB/04046/2020), and UIDP/04046/2020 (<https://doi.org/10.54499/UIDP/04046/2020>) Centre grants from FCT (to BioISI)]. P.J.d.C. was recipient of a fellowship from the BioSys PhD programme (SFRH/BD/52495/2014) and J.M. was a postdoc fellow (SFRH/BPD/98360/2013) from FCT. Work at ITQB-NOVA was financially supported by FCT, Project MOSTMICRO-ITQB with references UIDB/04612/2020 and UIDP/04612/2020, and LS4FUTURE Associated Laboratory (LA/P/0087/2020). M.S. is a recipient of FCT DL57.

**Institutional Review Board Statement:** Not applicable.

**Informed Consent Statement:** Not applicable.

**Data Availability Statement:** The data that support the findings of this study are available from the corresponding author upon reasonable request.

**Conflicts of Interest:** The authors declare no conflicts of interest.

## Appendix A

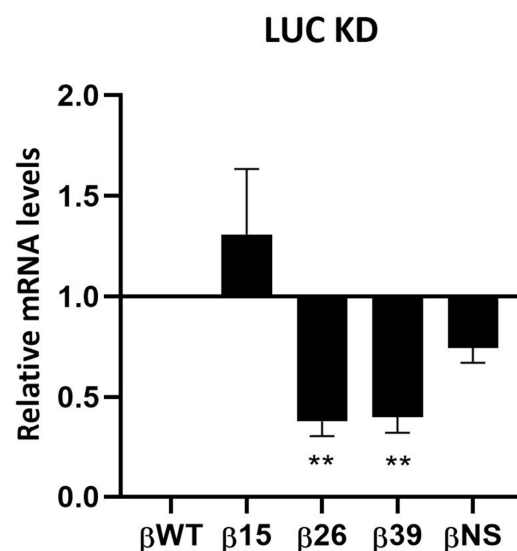


**Figure A1.** Real-time PCR (RT-qPCR) analysis of human  $\beta$ -globin mRNAs variants in HeLa cells transiently co-transfected with Luciferase (LUC) siRNA (Control). The y-axis represents mRNA fold change. The control (Luciferase KD) was normalized to a baseline of 1, and all other conditions are shown relative to this baseline. Values above 1 indicate upregulation, while values below 1 indicate downregulation. Asterisks (\*) indicate statistical significance relatively to the mRNA levels of the corresponding NMD target at control conditions. \*\*  $p < 0.01$ .

## References

1. Linde, L.; Kerem, B. Introducing sense into nonsense in treatments of human genetic diseases. *Trends Genet.* **2008**, *24*, 552–563. [[CrossRef](#)] [[PubMed](#)]
2. Bhuvanagiri, M.; Schlitter, A.M.; Hentze, M.W.; Kulozik, A.E. NMD: RNA biology meets human genetic medicine. *Biochem. J.* **2010**, *430*, 365–377. [[CrossRef](#)] [[PubMed](#)]
3. Fasken, M.B.; Corbett, A.H. Process or perish: Quality control in mRNA biogenesis. *Nat. Struct. Mol. Biol.* **2005**, *12*, 482–488. [[CrossRef](#)]
4. Klauer, A.A.; van Hoof, A. Degradation of mRNAs that lack a stop codon: A decade of nonstop progress. *Wiley Interdiscip. Rev. RNA* **2012**, *3*, 649–660. [[CrossRef](#)] [[PubMed](#)]
5. Schweingruber, C.; Rufener, S.C.; Zünd, D.; Yamashita, A.; Mühlemann, O. Nonsense-mediated mRNA decay—Mechanisms of substrate mRNA recognition and degradation in mammalian cells. *Biochim. Biophys. Acta-Gene Regul. Mech.* **2013**, *1829*, 612–623. [[CrossRef](#)]
6. Silva, A.L.; Romão, L. The mammalian nonsense-mediated mRNA decay pathway: To decay or not to decay! Which players make the decision? *FEBS Lett.* **2009**, *583*, 499–505. [[CrossRef](#)]
7. Mühlemann, O.; Jensen, T.H. mRNP quality control goes regulatory. *Trends Genet.* **2012**, *28*, 70–77. [[CrossRef](#)]
8. Saito, S.; Hosoda, N.; Hoshino, S.-I. The Hbs1-Dom34 protein complex functions in non-stop mRNA decay in mammalian cells. *J. Biol. Chem.* **2013**, *288*, 17832–17843. [[CrossRef](#)]
9. Mendell, J.T.; A Sharifi, N.; Meyers, J.L.; Martinez-Murillo, F.; Dietz, H.C. Nonsense surveillance regulates expression of diverse classes of mammalian transcripts and mutes genomic noise. *Nat. Genet.* **2004**, *36*, 1073–1078. [[CrossRef](#)]
10. Nicholson, P.; Yepiskoposyan, H.; Metze, S.; Orozco, R.Z.; Kleinschmidt, N.; Mühlemann, O. Nonsense-mediated mRNA decay in human cells: Mechanistic insights, functions beyond quality control and the double-life of NMD factors. *Cell. Mol. Life Sci.* **2009**, *67*, 677–700. [[CrossRef](#)]
11. Mühlemann, O.; Lykke-Andersen, J. How and where are nonsense mRNAs degraded in mammalian cells? *RNA Biol.* **2010**, *7*, 28–32. [[CrossRef](#)] [[PubMed](#)]
12. Huntzinger, E.; Kashima, I.; Fauser, M.; Saulière, J.; Izaurralde, E. SMG6 is the catalytic endonuclease that cleaves mRNAs containing nonsense codons in metazoan. *RNA* **2008**, *14*, 2609–2617. [[CrossRef](#)] [[PubMed](#)]
13. Eberle, A.B.; Lykke-Andersen, S.; Mühlemann, O.; Jensen, T.H. SMG6 promotes endonucleolytic cleavage of nonsense mRNA in human cells. *Nat. Struct. Mol. Biol.* **2009**, *16*, 49–55. [[CrossRef](#)]
14. Lejeune, F.; Li, X.; Maquat, L.E. Nonsense-mediated mRNA decay in mammalian cells involves decapping, deadenylation, and exonucleolytic activities. *Mol. Cell.* **2003**, *12*, 675–687. [[CrossRef](#)]
15. Chen, C.-Y.A.; Shyu, A.-B. Rapid deadenylation triggered by a nonsense codon precedes decay of the RNA body in a mammalian cytoplasmic nonsense-mediated decay pathway. *Mol. Cell Biol.* **2003**, *23*, 4805–4813. [[CrossRef](#)]
16. Couttet, P.; Grange, T. Premature termination codons enhance mRNA decapping in human cells. *Nucleic Acids Res.* **2004**, *32*, 488–494. [[CrossRef](#)] [[PubMed](#)]
17. Loh, B.; Jonas, S.; Izaurralde, E. The SMG5-SMG7 heterodimer directly recruits the CCR4-NOT deadenylase complex to mRNAs containing nonsense codons via interaction with POP2. *Genes Dev.* **2013**, *27*, 2125–2138. [[CrossRef](#)] [[PubMed](#)]
18. Lykke-Andersen, S.; Brodersen, D.E.; Jensen, T.H. Origins and activities of the eukaryotic exosome. *J. Cell Sci.* **2009**, *122*, 1487–1494. [[CrossRef](#)]
19. Mitchell, P.; Petfalski, E.; Shevchenko, A.; Mann, M.; Tollervey, D. The exosome: A conserved eukaryotic RNA processing complex containing multiple 3′ → 5′ exoribonucleases. *Cell* **1997**, *91*, 457–466. [[CrossRef](#)]
20. Allmang, C.; Petfalski, E.; Podtelejnikov, A.; Mann, M.; Tollervey, D.; Mitchell, P. The yeast exosome and human PM-Scl are related complexes of 3′ → 5′ exonucleases. *Genes Dev.* **1999**, *13*, 2148–2158. [[CrossRef](#)]
21. Liu, Q.; Greimann, J.C.; Lima, C.D. Reconstitution, Activities, and Structure of the Eukaryotic RNA Exosome. *Cell* **2006**, *127*, 1223–1237. [[CrossRef](#)] [[PubMed](#)]
22. Dziembowski, A.; Lorentzen, E.; Conti, E.; Séraphin, B. A single subunit, Dis3, is essentially responsible for yeast exosome core activity. *Nat. Struct. Mol. Biol.* **2007**, *14*, 15–22. [[CrossRef](#)] [[PubMed](#)]
23. Frazão, C.; McVey, C.E.; Amblar, M.; Barbas, A.; Vonrhein, C.; Arraiano, C.M.; Carrondo, M.A. Unravelling the dynamics of RNA degradation by ribonuclease II and its RNA-bound complex. *Nature* **2006**, *443*, 110–114. [[CrossRef](#)]
24. Zuo, Y.; Vincent, H.A.; Zhang, J.; Wang, Y.; Deutscher, M.P.; Malhotra, A. Structural Basis for Processivity and Single-Strand Specificity of RNase II. *Mol. Cell* **2006**, *24*, 149–156. [[CrossRef](#)] [[PubMed](#)]
25. Lebreton, A.; Tomecki, R.; Dziembowski, A.; Séraphin, B. Endonucleolytic RNA cleavage by a eukaryotic exosome. *Nature* **2008**, *456*, 993–996. [[CrossRef](#)]
26. Schaeffer, D.; Tsanova, B.; Barbas, A.; Reis, F.P.; Dastidar, E.G.; Sanchez-Rotunno, M.; Arraiano, C.M.; van Hoof, A. The exosome contains domains with specific endoribonuclease, exoribonuclease and cytoplasmic mRNA decay activities. *Nat. Struct. Mol. Biol.* **2009**, *16*, 56–62. [[CrossRef](#)]
27. Staals, R.H.J.; Bronkhorst, A.W.; Schilders, G.; Slomovic, S.; Schuster, G.; Heck, A.J.R.; Rajmakers, R.; Pruijn, G.J.M. Dis3-like 1, A novel exoribonuclease associated with the human exosome. *EMBO J.* **2010**, *29*, 2358–2367. [[CrossRef](#)]

28. Tomecki, R.; Kristiansen, M.S.; Lykke-Andersen, S.; Chlebowska, A.; Larsen, K.M.; Szczesny, R.J.; Drazkowska, K.; Pastula, A.; Andersen, J.S.; Stepien, P.P.; et al. The human core exosome interacts with differentially localized processive RNases: hDIS3 and hDIS3L. *EMBO J.* **2010**, *29*, 2342–2357. [[CrossRef](#)]
29. Ustianenko, D.; Hrossova, D.; Potesil, D.; Chalupnikova, K.; Hrazdilova, K.; Pachernik, J.; Cetkovska, K.; Uldrijan, S.; Zdrahal, Z.; Vanacova, S. Mammalian DIS3L2 exoribonuclease targets the uridylylated precursors of let-7 miRNAs. *RNA* **2013**, *19*, 1632–1638. [[CrossRef](#)]
30. Malecki, M.; Viegas, S.C.; Carneiro, T.; Golik, P.; Dressaire, C.; Ferreira, M.G.; Arraiano, C.M. The exoribonuclease Dis3L2 defines a novel eukaryotic RNA degradation pathway. *EMBO J.* **2013**, *32*, 1842–1854. [[CrossRef](#)]
31. Chang, H.-M.; Triboulet, R.; Thornton, J.E.; Gregory, R.I. A role for the Perlman syndrome exonuclease Dis3L2 in the Lin28-let-7 pathway. *Nature* **2013**, *497*, 244–248. [[CrossRef](#)] [[PubMed](#)]
32. Lim, J.; Ha, M.; Chang, H.; Kwon, S.C.; Simanshu, D.K.; Patel, D.J.; Kim, V.N. Uridylation by TUT4 and TUT7 marks mRNA for degradation. *Cell* **2014**, *159*, 1365–1376. [[CrossRef](#)]
33. Thomas, M.P.; Liu, X.; Whangbo, J.; McCrossan, G.; Sanborn, K.B.; Basar, E.; Walch, M.; Lieberman, J. Apoptosis Triggers Specific, Rapid, and Global mRNA Decay with 3' Uridylated Intermediates Degraded by DIS3L2. *Cell Rep.* **2015**, *11*, 1079–1089. [[CrossRef](#)] [[PubMed](#)]
34. Ustianenko, D.; Pasulka, J.; Feketova, Z.; Bednarik, L.; Zigackova, D.; Fortova, A.; Zavolan, M.; Vanacova, S. TUT-DIS3L2 is a mammalian surveillance pathway for aberrant structured non-coding RNAs. *EMBO J.* **2016**, *35*, 2179–2191. [[CrossRef](#)]
35. da Costa, P.J.; Menezes, J.; Saramago, M.; Garcia-Moreno, J.F.; Santos, H.A.; Gama-Carvalho, M.; Arraiano, C.M.; Viegas, S.C.; Romão, L. A role for DIS3L2 over natural nonsense-mediated mRNA decay targets in human cells. *Biochem. Biophys. Res. Commun.* **2019**, *518*, 664–671. [[CrossRef](#)]
36. Kurosaki, T.; Miyoshi, K.; Myers, J.R.; Maquat, L.E. NMD-degradome sequencing reveals ribosome-bound intermediates with 3'-end non-templated nucleotides. *Nat. Struct. Mol. Biol.* **2018**, *25*, 940. [[CrossRef](#)]
37. Romão, L.; Inácio, A.; Santos, S.; Ávila, M.; Faustino, P.; Pacheco, P.; Lavinha, J. Nonsense mutations in the human  $\beta$ -globin gene lead to unexpected levels of cytoplasmic mRNA accumulation. *Blood* **2000**, *96*, 2895–2902. [[CrossRef](#)] [[PubMed](#)]
38. Inácio, A.; Silva, A.L.; Pinto, J.; Ji, X.; Morgado, A.; Almeida, F.; Faustino, P.; Lavinha, J.; Liebhaber, S.A.; Romão, L. Nonsense mutations in close proximity to the initiation codon fail to trigger full nonsense-mediated mRNA decay. *J. Biol. Chem.* **2004**, *279*, 32170–32180. [[CrossRef](#)]
39. Silva, A.L.; Ribeiro, P.; Inácio, A.; Liebhaber, S.A.; Romão, L. Proximity of the poly(A)-binding protein to a premature termination codon inhibits mammalian nonsense-mediated mRNA decay. *RNA* **2008**, *14*, 563–576. [[CrossRef](#)]
40. da Costa, P.J.; Menezes, J.; Saramago, M.; Garcia-Moreno, J.F.; Santos, H.A.; Gama-Carvalho, M.; Arraiano, C.M.; Viegas, S.C.; Romão, L. A role for DIS3L2 over human nonsense-mediated mRNA decay targets. *bioRxiv* **2019**. [[CrossRef](#)]
41. Brogna, S.; McLeod, T.; Petric, M. The Meaning of NMD: Translate or Perish. *Trends Genet.* **2016**, *32*, 395–407. [[CrossRef](#)] [[PubMed](#)]
42. Hug, N.; Cáceres, J.F. The RNA Helicase DHX34 Activates NMD by promoting a transition from the surveillance to the decay-inducing complex. *Cell Rep.* **2014**, *8*, 1845–1856. [[CrossRef](#)] [[PubMed](#)]
43. Karousis, E.D.; Nasif, S.; Mühlemann, O. Nonsense-mediated mRNA decay: Novel mechanistic insights and biological impact. *Wiley Interdiscip. Rev. RNA* **2016**, *7*, 661–682. [[CrossRef](#)]
44. Saveanu, C.; Jacquier, A. How cells kill a “killer” messenger. *eLife* **2016**, *5*, e16076. [[CrossRef](#)]
45. Celik, A.; Baker, R.; He, F.; Jacobson, A. High-resolution profiling of NMD targets in yeast reveals translational fidelity as a basis for substrate selection. *RNA* **2017**, *23*, 735–748. [[CrossRef](#)]
46. Karousis, E.D.; Mühlemann, O. Nonsense-Mediated mRNA Decay Begins where Translation Ends. *Cold Spring Harb. Perspect. Biol.* **2019**, *11*, a032862. [[CrossRef](#)] [[PubMed](#)]
47. Raimondeau, E.; Bufton, J.C.; Schaffitzel, C. New insights into the interplay between the translation machinery and nonsense-mediated mRNA decay factors. *Biochem. Soc. Trans.* **2018**, *46*, 503–512. [[CrossRef](#)]
48. Kim, Y.K.I.; Maquat, L.E. UPFront and center in RNA decay: UPF1 in nonsense-mediated mRNA decay and beyond. *RNA* **2019**, *25*, 407–422. [[CrossRef](#)]
49. Tani, H.; Imamachi, N.; Salam, K.A.; Mizutani, R.; Ijiri, K.; Irie, T.; Yada, T.; Suzuki, Y.; Akimitsu, N. Identification of hundreds of novel UPF1 target transcripts by direct determination of whole transcriptome stability. *RNA Biol.* **2012**, *9*, 1370–1379. [[CrossRef](#)]
50. Boehm, V.; Kueckelmann, S.; Gerbracht, J.V.; Kallabis, S.; Britto-Borges, T.; Altmüller, J.; Krüger, M.; Dieterich, C.; Gehring, N.H. SMG5-SMG7 authorize nonsense-mediated mRNA decay by enabling SMG6 endonucleolytic activity. *Nat. Commun.* **2021**, *12*, 1–19. [[CrossRef](#)]
51. Yamashita, A. Role of SMG-1-mediated Upf1 phosphorylation in mammalian nonsense-mediated mRNA decay. *Genes Cells* **2013**, *18*, 161–175. [[CrossRef](#)] [[PubMed](#)]
52. Nath, P.; Alfarsi, L.H.; El-Ansari, R.; Masisi, B.K.; Erkan, B.; Fakroun, A.; Ellis, I.O.; Rakha, E.A.; Green, A.R. The amino acid transporter SLC7A11 expression in breast cancer. *Cancer Biol. Ther.* **2024**, *25*, 2291855. [[CrossRef](#)]
53. Andersen, J.V.; Markussen, K.H.; Jakobsen, E.; Schousboe, A.; Waagepetersen, H.S.; Rosenberg, P.A.; Aldana, B.I. Glutamate metabolism and recycling at the excitatory synapse in health and neurodegeneration. *Neuropharmacology* **2021**, *196*, 108719. [[CrossRef](#)]
54. Tamura, R.E.; De Vasconcellos, J.F.; Sarkar, D.; Libermann, T.A.; Fisher, P.B.; Zerbini, L.F. GADD45 proteins: Central players in tumorigenesis. *Curr. Mol. Med.* **2012**, *12*, 634–651. [[CrossRef](#)]

55. Hervouet, E.; Claude-Taupin, A.; Gauthier, T.; Perez, V.; Fraichard, A.; Adami, P.; Despouy, G.; Monnien, F.; Algros, M.-P.; Jouvenot, M.; et al. The autophagy *GABARAPL1* gene is epigenetically regulated in breast cancer models. *BMC Cancer* **2015**, *15*, 729. [[CrossRef](#)]
56. Huang, X.; Zhang, J.; Zheng, Y. ANTXR1 Is a Prognostic Biomarker and Correlates with Stromal and Immune Cell Infiltration in Gastric Cancer. *Front. Mol. Biosci.* **2020**, *7*, 598221. [[CrossRef](#)]
57. Hai, T.; Wolfgang, C.D.; Marsee, D.K.; Allen, A.E.; Sivaprasad, U. ATF3 and Stress Responses. *Gene Expr.* **1999**, *7*, 321.
58. Hommel, A.; Hesse, D.; Völker, W.; Jaschke, A.; Moser, M.; Engel, T.; Blüher, M.; Zahn, C.; Chadt, A.; Ruschke, K.; et al. The ARF-like GTPase ARFRP1 is essential for lipid droplet growth and is involved in the regulation of lipolysis. *Mol. Cell Biol.* **2010**, *30*, 1231–1242. [[CrossRef](#)]
59. Cutress, R.I.; Townsend, P.A.; Brimmell, M.; Bateman, A.C.; Hague, A.; Packham, G. BAG-1 expression and function in human cancer. *Br. J. Cancer* **2002**, *87*, 834–839. [[CrossRef](#)] [[PubMed](#)]
60. Boehm, V.; Haberman, N.; Ottens, F.; Ule, J.; Gehring, N.H. 3' UTR length and messenger ribonucleoprotein composition determine endocleavage efficiencies at termination codons. *Cell Rep.* **2014**, *9*, 555–568. [[CrossRef](#)]
61. Schmidt, S.A.; Foley, P.L.; Jeong, D.-H.; Rymarquis, L.A.; Doyle, F.; Tenenbaum, S.A.; Belasco, J.G.; Green, P.J. Identification of SMG6 cleavage sites and a preferred RNA cleavage motif by global analysis of endogenous NMD targets in human cells. *Nucleic Acids Res.* **2015**, *43*, 309–323. [[CrossRef](#)] [[PubMed](#)]
62. Colombo, M.; Karousis, E.D.; Bourquin, J.; Bruggmann, R.; Mühlemann, O. Transcriptome-wide identification of NMD-targeted human mRNAs reveals extensive redundancy between SMG6- and SMG7-mediated degradation pathways. *RNA* **2017**, *23*, 189–201. [[CrossRef](#)] [[PubMed](#)]
63. Ottens, F.; Boehm, V.; Sibley, C.R.; Ule, J.; Gehring, N.H. Transcript-specific characteristics determine the contribution of endo- and exonucleolytic decay pathways during the degradation of nonsense-mediated decay substrates. *RNA* **2017**, *23*, 1224–1236. [[CrossRef](#)]
64. Metzke, S.; Herzog, V.A.; Ruepp, M.-D.; Mühlemann, O. Comparison of EJC-enhanced and EJC-independent NMD in human cells reveals two partially redundant degradation pathways. *RNA* **2013**, *19*, 1432–1448. [[CrossRef](#)] [[PubMed](#)]
65. Nicholson, P.; Josi, C.; Kurosawa, H.; Yamashita, A.; Mühlemann, O. A novel phosphorylation-independent interaction between SMG6 and UPF1 is essential for human NMD. *Nucleic Acids Res.* **2014**, *42*, 9217–9235. [[CrossRef](#)]
66. Gatfield, D.; Izaurrealde, E. Nonsense-mediated messenger RNA decay is initiated by endonucleolytic cleavage in *Drosophila*. *Nature* **2004**, *429*, 575–578. [[CrossRef](#)]
67. Schaeffer, D.; van Hoof, A. Different nuclease requirements for exosome-mediated degradation of normal and nonstop mRNAs. *Proc. Natl. Acad. Sci. USA* **2011**, *108*, 2366–2371. [[CrossRef](#)]
68. Jamar, N.H.; Kritsiligkou, P.; Grant, C.M. The non-stop decay mRNA surveillance pathway is required for oxidative stress tolerance. *Nucleic Acids Res.* **2017**, *45*, 6881–6893. [[CrossRef](#)]
69. Robinson, S.R.; Oliver, A.W.; Chevassut, T.J.; Newbury, S.F. The 3' to 5' Exoribonuclease DIS3, From Structure and Mechanisms to Biological Functions and Role in Human Disease. *Biomolecules* **2015**, *5*, 1515–1539. [[CrossRef](#)]
70. Szczepińska, T.; Kalisiak, K.; Tomecki, R.; Labno, A.; Borowski, L.S.; Kulinski, T.M.; Adamska, D.; Kosinska, J.; Dziembowski, A. DIS3 shapes the RNA polymerase II transcriptome in humans by degrading a variety of unwanted transcripts. *Genome Res.* **2015**, *25*, 1622–1633. [[CrossRef](#)]
71. Andrusis, E.D.; Werner, J.; Nazarian, A.; Erdjument-Bromage, H.; Tempst, P.; Lis, J.T. The RNA processing exosome is linked to elongating RNA polymerase II in *Drosophila*. *Nature* **2002**, *420*, 837–841. [[CrossRef](#)] [[PubMed](#)]
72. Hesse, V.; Björk, P.; Sokolowski, M.; de Valdivia, E.G.; Silverstein, R.; Artemenko, K.; Tyagi, A.; Maddalo, G.; Ilag, L.; Helbig, R.; et al. The exosome associates cotranscriptionally with the nascent pre-mRNP through interactions with heterogeneous nuclear ribonucleoproteins. *Mol. Biol. Cell* **2009**, *20*, 3459–3470. [[CrossRef](#)] [[PubMed](#)]
73. van Hoof, A.; Lennertz, P.; Parker, R. Yeast Exosome Mutants Accumulate 3'-Extended Polyadenylated Forms of U4 Small Nuclear RNA and Small Nucleolar RNAs. *Mol. Cell Biol.* **2000**, *20*, 441–452. [[CrossRef](#)]
74. Januszyk, K.; Lima, C.D. The eukaryotic RNA exosome. *Curr. Opin. Struct. Biol.* **2014**, *24*, 132–140. [[CrossRef](#)] [[PubMed](#)]
75. van Dijk, E.L.; Schilders, G.; Pruijn, G.J.M. Human cell growth requires a functional cytoplasmic exosome, which is involved in various mRNA decay pathways. *RNA* **2007**, *13*, 1027–1035. [[CrossRef](#)]
76. Wasmuth, E.V.; Lima, C.D. The Rps6 C-terminal domain binds RNA and activates the nuclear RNA exosome. *Nucleic Acids Res.* **2017**, *45*, 846–860. [[CrossRef](#)]
77. Wasmuth, E.V.; Lima, C.D. Structure and Activities of the Eukaryotic RNA Exosome. In *The Enzymes*; Academic Press: Cambridge, MA, USA, 2012; pp. 53–75. [[CrossRef](#)]
78. Wasmuth, E.V.; Lima, C.D. Exo- and endoribonucleolytic activities of yeast cytoplasmic and nuclear RNA exosomes are dependent on the noncatalytic core and central channel. *Mol. Cell* **2012**, *48*, 133–144. [[CrossRef](#)]
79. Haimovich, G.; Medina, D.A.; Causse, S.Z.; Garber, M.; Millán-Zambrano, G.; Barkai, O.; Chávez, S.; Pérez-Ortín, J.E.; Darzacq, X.; Choder, M. Gene expression is circular: Factors for mRNA degradation also foster mRNA synthesis. *Cell* **2013**, *153*, 1000–1011. [[CrossRef](#)]
80. Sun, M.; Schwalb, B.; Pirkl, N.; Maier, K.C.; Schenk, A.; Failmezger, H.; Tresch, A.; Cramer, P. Global analysis of eukaryotic mRNA degradation reveals Xrn1-dependent buffering of transcript levels. *Mol. Cell* **2013**, *52*, 52–62. [[CrossRef](#)]

81. Jones, C.I.; Zabolotskaya, M.V.; Newbury, S.F. The 5' → 3' exoribonuclease XRN1/Pacman and its functions in cellular processes and development. *Wiley Interdiscip. Rev. RNA* **2012**, *3*, 455–468. [[CrossRef](#)]
82. Łabno, A.; Tomecki, R.; Dziembowski, A. Cytoplasmic RNA decay pathways—Enzymes and mechanisms. *Biochim. Biophys. Acta (BBA)-Mol. Cell Res.* **2016**, *1863*, 3125–3147. [[CrossRef](#)]
83. Moon, S.L.; Blackinton, J.G.; Anderson, J.R.; Dozier, M.K.; Dodd, B.J.T.; Keene, J.D.; Wilusz, C.J.; Bradrick, S.S.; Wilusz, J. XRN1 stalling in the 5' UTR of Hepatitis C virus and Bovine Viral Diarrhea virus is associated with dysregulated host mRNA stability. *PLoS Pathog.* **2015**, *11*, e1004708. [[CrossRef](#)] [[PubMed](#)]
84. MacFadden, A.; O'donoghue, Z.; Silva, P.A.G.C.; Chapman, E.G.; Olsthoorn, R.C.; Sterken, M.G.; Pijlman, G.P.; Bredenbeek, P.J.; Kieft, J.S. Mechanism and structural diversity of exoribonuclease-resistant RNA structures in flaviviral RNAs. *Nat. Commun.* **2018**, *9*, 119. [[CrossRef](#)] [[PubMed](#)]
85. Vaché, C.; Cubedo, N.; Mansard, L.; Sarniguet, J.; Baux, D.; Faugère, V.; Baudoin, C.; Moclyn, M.; Touraine, R.; Lina-Granade, G.; et al. Identification and in vivo functional investigation of a HOMER2 nonstop variant causing hearing loss. *Eur. J. Hum. Genet.* **2023**, *31*, 834–840. [[CrossRef](#)]
86. Terrey, M.; I Adamson, S.; Chuang, J.H.; Ackerman, S.L.; Neurobiology, S.O.; States, U. Defects in translation-dependent quality control pathways lead to convergent molecular and neurodevelopmental pathology. *eLife* **2021**, *10*, e66904. [[CrossRef](#)]

**Disclaimer/Publisher's Note:** The statements, opinions and data contained in all publications are solely those of the individual author(s) and contributor(s) and not of MDPI and/or the editor(s). MDPI and/or the editor(s) disclaim responsibility for any injury to people or property resulting from any ideas, methods, instructions or products referred to in the content.